


ARTICLE

<https://doi.org/10.1038/s41467-019-08869-9>

OPEN

A platform for glycoengineering a polyvalent pneumococcal bioconjugate vaccine using *E. coli* as a host

Christian M. Harding¹, Mohamed A. Nasr^{2,7}, Nichollas E. Scott³, Guillaume Goyette-Desjardins ⁴, Harald Nothhaft², Anne E. Mayer⁵, Sthefany M. Chavez⁵, Jeremy P. Huynh⁵, Rachel L. Kinsella⁵, Christine M. Szymanski⁶, Christina L. Stallings⁵, Mariela Segura⁴ & Mario F. Feldman^{1,5}

Chemical synthesis of conjugate vaccines, consisting of a polysaccharide linked to a protein, can be technically challenging, and in vivo bacterial conjugations (bioconjugations) have emerged as manufacturing alternatives. Bioconjugation relies upon an oligosaccharyl-transferase to attach polysaccharides to proteins, but currently employed enzymes are not suitable for the generation of conjugate vaccines when the polysaccharides contain glucose at the reducing end, which is the case for ~75% of *Streptococcus pneumoniae* capsules. Here, we use an O-linking oligosaccharyltransferase to generate a polyvalent pneumococcal bioconjugate vaccine with polysaccharides containing glucose at their reducing end. In addition, we show that different vaccine carrier proteins can be glycosylated using this system. Pneumococcal bioconjugates are immunogenic, protective and rapidly produced within *E. coli* using recombinant techniques. These proof-of-principle experiments establish a platform to overcome limitations of other conjugating enzymes enabling the development of bioconjugate vaccines for many important human and animal pathogens.

¹VaxNewMo LLC, St. Louis, MO 63108, USA. ²Department of Biological Sciences, University of Alberta, Edmonton, AB T6G 2R3, Canada. ³Department of Microbiology and Immunology, Institute for Infection and Immunity, University of Melbourne at the Peter Doherty, Parkville, VIC 3010, Australia. ⁴Swine and Poultry Infectious Diseases Research Center, Faculty of Veterinary Medicine, University of Montreal, 3200 Sicotte Street, St-Hyacinthe, QC J2S 2M2, Canada. ⁵Department of Molecular Microbiology, Washington University School of Medicine, St Louis, MO 63110, USA. ⁶Department of Microbiology and Complex Carbohydrate Research Center, University of Georgia, Athens, GA 30602, USA. ⁷Present address: Department of Biology, Centre for Applied Synthetic Biology, Concordia University, Montreal, QC H4B 1R6, Canada. These authors contributed equally: Christian M. Harding, Mohamed A. Nasr. Correspondence and requests for materials should be addressed to C.M.H. (email: christian.harding@vaxnewmo.com) or to M.F.F. (email: mariofeldman@wustl.edu)

S*treptococcus pneumoniae* (pneumococcus) is a leading cause of bacterial-induced pneumonia, meningitis, and bacteremia globally, particularly, afflicting children 5 years of age or younger^{1,2}. Moreover, a 2000 epidemiological survey from the World Health Organization (WHO) estimated that 735,000 human immunodeficiency virus-uninfected children died from pneumococcal-related diseases² with updated estimates slightly reduced to 541,000 deaths for the year 2008 (ref. ³). An increase in the number of prophylactic treatment options, mainly due to advancements in pneumococcal vaccine developments, has emerged over the past two decades. Pneumovax[®]23, a 23-valent polysaccharide vaccine, is used in elderly populations as well as children over the age of 2 years who are at increased risk of pneumococcal disease⁴; however, polysaccharide vaccines typically act as T cell-independent antigens and are generally not effective in children 2 years of age and younger⁵. On the other hand, covalently linking a polysaccharide to a protein in the form of a conjugate vaccine elicits a T cell-dependent immune response across all age groups, characterized by high-affinity immunoglobulin G (IgG)-producing plasma cells and memory B cells^{6,7}.

Three pneumococcal conjugate vaccines have been commercially licensed since the year 2000: Prevnar[®], Synflorix[™], and Prevnar 13[®]. Prevnar 13[®], the most broadly protecting pneumococcal conjugate vaccine, is comprised of 13 protein-polysaccharide conjugates consisting of pneumococcal serotypes 1, 3, 4, 5, 6A, 6B, 7F, 9V, 14, 18C, 19A, 19F, and 23F, each individually linked to the genetically inactivated diphtheria toxoid CRM₁₉₇. Although highly protective in a three-dose schedule, Prevnar 13[®] is one of the most expensive vaccines on the market today. This is mainly due to its complex manufacturing process resulting in a cost of ~600 US dollars for primary and booster immunizations⁸. In fact, Prevnar 13[®] has been Pfizer's best-selling product for the fiscal years 2015–2017, with total revenues exceeding 17.5 billion US dollars⁹. Although pneumococcal conjugate vaccines have significantly reduced the burden of pneumococcal disease events^{10,11}, due to variations in global serotype distributions^{12,13}, serotype replacement events¹⁴, as well as the lack of a low-cost alternative for developing countries, alternative manufacturing strategies to expedite development of next generation vaccines are needed.

As mentioned above, currently licensed pneumococcal conjugate vaccines are synthesized chemically, which is a laborious process plagued with technical challenges, low yields, and batch-to-batch variations¹⁵, highlighting the need for improved conjugate vaccine synthetic methodologies. Over the past 15 years, *in vivo* conjugation using bacterial protein glycosylation systems has emerged as a feasible alternative to chemical conjugation¹⁶, with multiple bioconjugate vaccine candidates now in various stages of development and clinical trials^{17,18}. Bioconjugation is based on exploiting protein glycosylation, a ubiquitous post-translational modification in which glycans are covalently linked to proteins. In bacteria, glycans are commonly bound to proteins via *N*- or *O*-linkages on asparagine or serine/threonine residues, respectively^{19,20}. Several pathways for bacterial glycosylation have been characterized, and among the best described are the oligosaccharyltransferase (OTase)-dependent pathways in Gram-negative bacteria²⁰. In these systems, a lipid-linked oligosaccharide is assembled sequentially at the cytoplasmic leaflet of the inner membrane, flipped to the periplasmic leaflet, and then transferred to acceptor proteins by either *N*- or *O*-OTases depending on the site of glycan attachment²⁰. Many bacterial species, including *S. pneumoniae*, also synthesize capsular polysaccharides (CPSs) employing the same lipid-linked oligosaccharides prior to their polymerization, export, and transfer to the cell surface enabling their exploitation for bioconjugation reactions in *Escherichia coli*²¹.

Glycoproteins have been recombinantly synthesized in *E. coli* for use as vaccines¹⁶ and/or diagnostics^{22,23} by co-expressing three components: a genetic cluster encoding for the proteins required to synthesize a glycan of interest, an OTase and an acceptor protein. One drawback of this process is the apparent glycan substrate specificity of the known OTases, which, for some of them, has been suggested to be dictated by the reducing end sugar²⁴ (the first monosaccharide in the growing polysaccharide chain) of the lipid-linked oligo/polysaccharide of interest. Although OTases are able to transfer many different oligo- and polysaccharide structures^{24,25}, some sugars have not been efficiently conjugated by known OTases to acceptor proteins. Therefore, characterizing different OTases is paramount for expanding our arsenal of therapeutic glycoproteins, including bioconjugate vaccines.

OTases currently used for commercially synthesizing glycoconjugates are the *Campylobacter jejuni* *N*-OTase PglB¹⁶ and the *Neisseria meningitidis* *O*-OTase PglL²⁶, both of which exhibit a great deal of promiscuity towards glycan substrates^{24,25}. However, neither enzyme has been experimentally demonstrated to conjugate glycans containing a glucose residue at the reducing end, such as ~75% of *S. pneumoniae* CPSs^{19,27}. In the present work, we demonstrate the first successful *in vivo* conjugation of *S. pneumoniae* CPSs containing glucose as the reducing end monosaccharide from multiple serotypes. This has been achieved using a different class of *O*-OTase, previously designated as PglL_{Comp} by our group²⁸, and henceforth termed PglS. Here, we present proof-of-concept studies on the engineering, characterization, and immunological responses of a polyvalent pneumococcal bioconjugate vaccine using the natural acceptor protein ComP as a vaccine carrier as well as a monovalent pneumococcal bioconjugate vaccine using a conventional vaccine carrier containing the *Pseudomonas aeruginosa* exotoxin A protein.

Results

PglS transfers pneumococcal CPS14 to its acceptor protein.

PglB, the first OTase described, was shown to preferentially transfer glycans containing an acetamido group at the C-2 position of the reducing end sugar to asparagine residues of acceptor proteins²⁴. However, polysaccharides with galactose (Gal) at the reducing end, such as the *Salmonella enterica* Typhimurium O antigen, have been transferred by an engineered PglB variant²⁹ and also by PglL, the *O*-OTase from *Neisseria meningitidis*²⁵. However, there is no evidence available for PglB- or PglL-mediated transfer of polysaccharides containing glucose (Glc) at the reducing end. We therefore tested the ability of PglB and PglL to transfer the pneumococcal CPS14, which has a Glc residue as the reducing end sugar, to their cognate acceptor proteins, AcrA and DsbA, respectively. As seen in Fig. 1a–f, no evidence for CPS14 glycosylation to either acceptor protein was observed.

Previously, we demonstrated that *Acinetobacter* species contain three *O*-linked OTases: a general PglL OTase responsible for glycosylating multiple proteins, and two pilin-specific OTases²⁸. The first pilin-specific OTase is an ortholog of TfpO (also known as PilO) and is not employed for *in vivo* conjugation systems due to its inability to transfer polysaccharides with more than one repeating unit²⁶. The second pilin-specific OTase, PglS, glycosylates a single protein, the type IV pilin ComP²⁸. A bioinformatic analysis indicated that PglS is the archetype of a distinct family of OTases, which prompted us to test its ability to transfer pneumococcal CPS14 to ComP. Western blotting analysis (Fig. 1g–i) showed that co-expression of the CPS14 biosynthetic locus in conjunction with PglS and a His-tagged variant of ComP resulted in a typical ladder-like pattern of bands compatible with protein glycosylation with multiple subunits. Both ComP-His (Fig. 1g) and CPS14 (Fig. 1h) were detected with antisera specific

to each antigen; moreover, samples treated with proteinase K did not react with either the anti-His or anti-CPS14 antisera, indicating that the purified material is indeed proteinaceous. Together, these results suggest that, unlike the previously characterized OTases, PglS is able to transfer polysaccharides with Glc at the reducing end.

ComP is glycosylated at a serine residue in position 84. *N*-glycosylation in bacteria generally occurs within the sequon D-X-N-S-T, where X is any amino acid but proline³⁰. On the contrary, *O*-linked OTases do not seem to have defined recognition sequons. Most *O*-glycosylation events in bacterial proteins occur in regions of low complexity (LCR), rich in serine, alanine, and proline residues^{31,32}. Some pilins are also *O*-glycosylated at a C-

terminal serine residue³³. We were unable to find an obvious LCR or a C-terminal serine residue in ComP homologous to those found in other pilin-like proteins and therefore employed mass spectrometry to determine the site(s) of glycosylation. Purified CPS14-ComP bioconjugates were subjected to GluC proteolytic digestion and multiple mass spectrometric analyses. As seen in Fig. 2, we identified a single glycopeptide consisting of a semi-GluC-derived peptide $_{81}\text{ISASNATTNVATAT}_{94}$ attached to a glycan that matched the published CPS14 composition (Fig. 2a). To enable the confirmation of both the peptide and attached glycan sequences, multiple collision energies regimens were performed to confirm the glycosylation of the semi-GluC-derived peptide $_{81}\text{ISASNATTNVATAT}_{94}$ with a 1378.47 Da glycan corresponding to HexNAc₂Hexose₆ (Fig. 2b). Additional glycopeptides were also observed decorated with extended glycans corresponding to up to four tetrasaccharide repeat units (Supplemental Fig. 1).

We have previously shown that *Acinetobacter* species predominantly glycosylate proteins at serine residues and thus hypothesized that either serine 82 or 84 was the site of glycosylation³². To determine which serine residue was the site of glycan attachment, we employed the *C. jejuni* heptasaccharide as the donor glycan, due to the ease at which glycosylation is detectable from whole-cell lysates. Wild-type ComP was glycosylated with the *C. jejuni* heptasaccharide as indicated by its increased electrophoretic mobility and signal co-localization with hR6 anti-glycan sera when co-expressed with PglS (Supplemental Fig. 2a-c). Mass spectrometry (MS) analysis also confirmed the presence of the *C. jejuni* heptasaccharide on the identical semi-GluC-derived peptide $_{81}\text{ISASNATTNVATAT}_{94}$ modified by CPS14 (Supplemental Figs. 3 and 4). As a negative control, we generated a catalytically inactive PglS mutant (H324A), which when co-expressed with the *C. jejuni* heptasaccharide glycan was unable to glycosylate wild-type ComP (Supplemental Fig. 2A-C). We next performed site-directed mutagenesis and observed that glycosylation of ComP with the *C. jejuni* heptasaccharide was abolished in the ComP[S84A] mutant, whereas ComP[S82A] was glycosylated at wild-type levels (Supplemental Fig. 2A-C). In addition, the site of ComP glycosylation was also determined using a pneumococcal polysaccharide and is discussed below.

Immunogenicity of a monovalent CPS14-ComP bioconjugate.

We evaluated the immunogenicity of a CPS14-ComP bioconjugate in a murine vaccination model. Two groups of mice ($n = 10$) individually received 3 μg of either unglycosylated ComP or CPS14-ComP bioconjugate. Mice were boosted on days 14 and 28, and sacrificed on day 49 for whole-blood collection. Each vaccine was formulated based on total protein. Using an enzyme-linked immunosorbent assay (ELISA) with a serotype 14 strain of *S. pneumoniae* adsorbed to each well, we compared IgM and IgG responses to CPS14. As seen in Supplemental Fig. 5, sera collected from mice vaccinated with a CPS14-ComP bioconjugate had an increased IgG response specific to CPS14 (Supp. Figure 5B), but not an increased IgM response (Supp. Figure 5A). Further, we employed secondary horseradish peroxidase (HRP)-tagged anti-IgG subtype antibodies to determine which of the IgG subtypes were present in CPS14-ComP-vaccinated mice (Supp. Figure 5C). We determined that the CPS14-specific IgG1 response was higher than the other subtypes, which is consistent with previous findings for pneumococcal conjugate vaccines^{34,35}.

Immunogenicity of a trivalent pneumococcal bioconjugate.

There are more than 90 serotypes of *S. pneumoniae*^{21,27}. Many increasingly prevalent serotypes, like serotypes 8, 22F, and 33F, are not included in currently licensed vaccines³⁶. Therefore, we

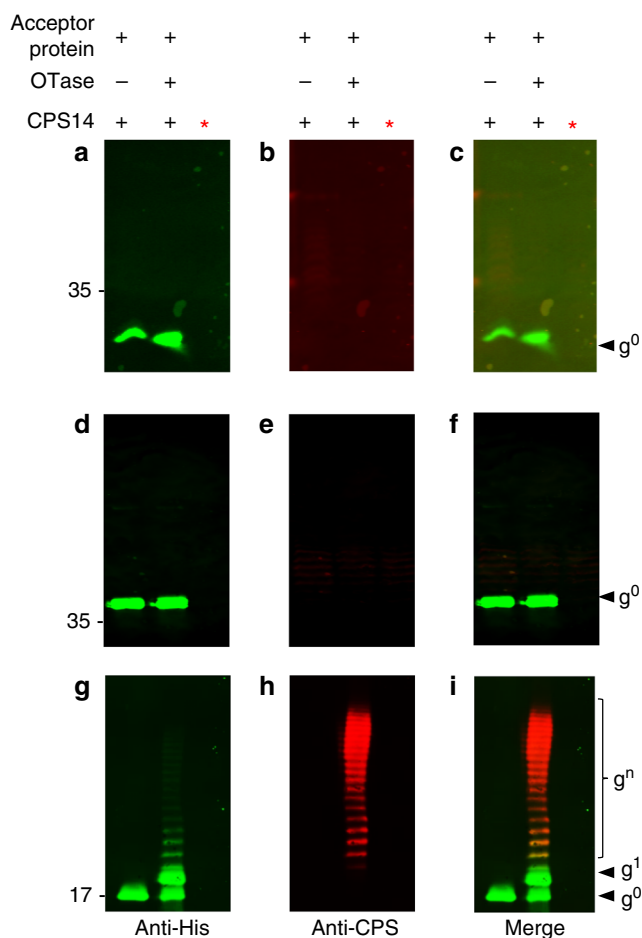


Fig. 1 PglS can glycosylate the acceptor protein ComP with the pneumococcal CPS14 polysaccharide. *Escherichia coli* SDB1 cells co-expressing an acceptor protein (DsbA, AcrA, or ComP), an OTase (PglL, PglB, or PglS), and the CPS14 polysaccharide were analyzed for protein glycosylation via western blot analysis of the affinity-purified acceptor proteins. **a-c** DsbA purified from SDB1 cells in the presence or absence of PglL. **a** Anti-His channel probing for Hexa-histidine tagged DsbA. **b** Anti-glycan channel probing for CPS14. **c** Merged images for panels a and b. **d-f** AcrA purified from SDB1 cells in the presence or absence of PglB. **d** Anti-His channel probing for Hexa-histidine tagged AcrA. **e** Anti-glycan channel probing for CPS14. **f** Merged images for panels d and e. **g-i** ComP purified from SDB1 cells in the presence or absence of PglS. **g** Anti-His channel probing for Hexa-histidine-tagged ComP. **h** Anti-glycan channel probing for CPS14. **i** Merged images for panels g and h. The red asterisk indicates samples that were proteinase K treated for 1 h at 55 °C. Source data are provided as a Source Data file

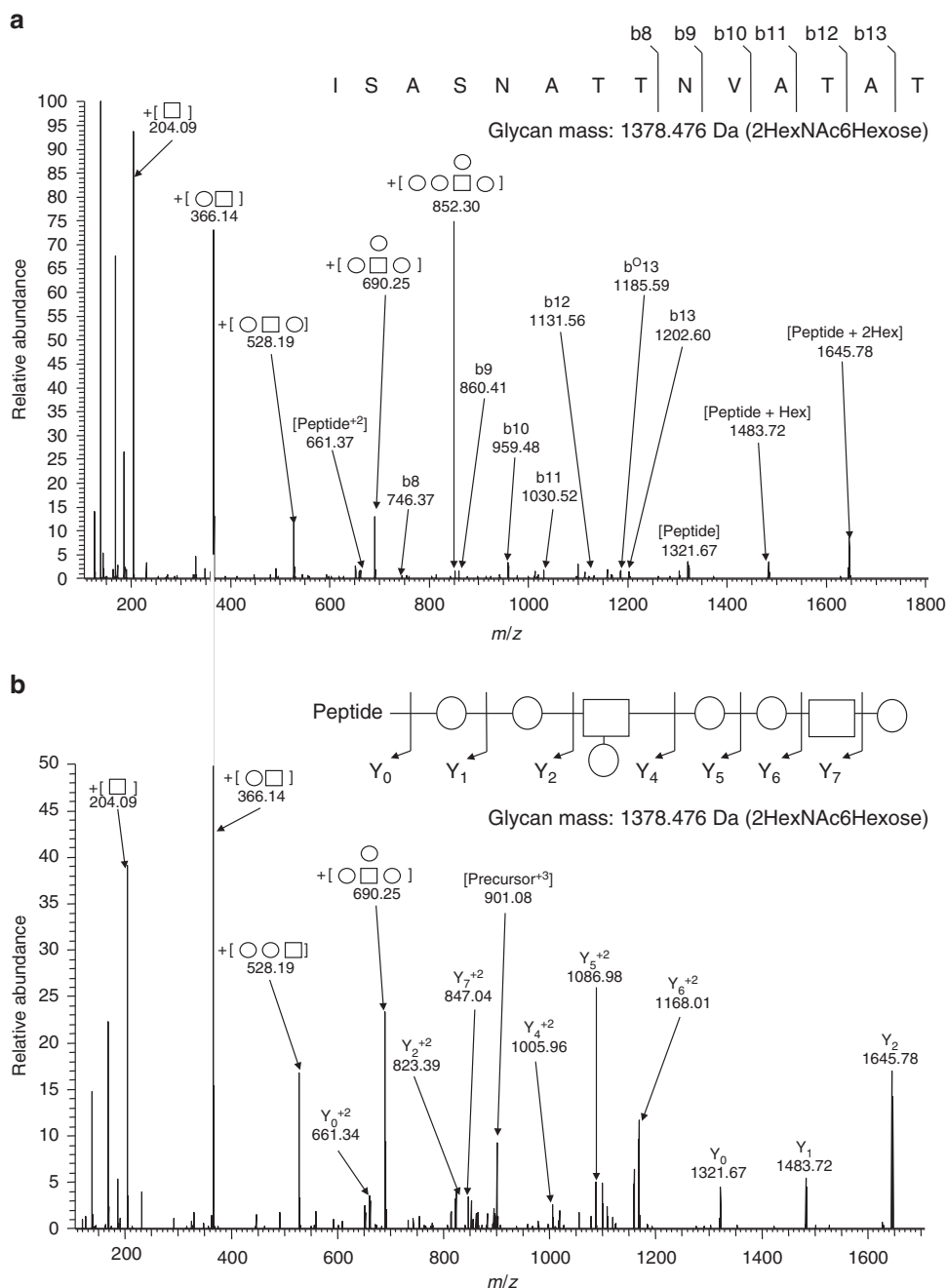


Fig. 2 Higher energy collisional dissociation (HCD) fragmentation spectra of GluC-digested CPS14-ComP bioconjugates. GluC-digested CPS14-ComP was subjected to HCD fragmentation enabling the confirmation of a single peptide attached to a glycan with the CPS14 repeating subunit. High collision energies (**a**) and low collision energies (**b**) regimens were undertaken to confirm the glycosylation of the peptide $_{81}$ ISASNATTNVATAT $_{94}$ with a 1378.47 Da glycan corresponding to HexNAc₂Hexose₆

tested the versatility of PglS to generate a multivalent pneumococcal bioconjugate vaccine against two serotypes included in Pevnar 13[®] (serotypes 9V and 14) and one serotype not included (serotype 8). The aforementioned CPSs all contain Glc as the reducing end sugar and are therefore not compatible with other commercially exploited conjugating enzymes. As seen in Figs. 3a-c and 3d-f, western blot analyses of affinity-purified proteins from whole cells co-expressing PglS, ComP, and either the CPS8 or CPS9V polysaccharides resulted in the generation CPS-specific ComP bioconjugates, respectively. Again, to confirm that the material purified was not contaminated with lipid-linked polysaccharides, we treated the samples with proteinase K and

observed a loss of signal when analyzed via western blotting, confirming that the bioconjugates were proteinaceous.

Next, we performed a vaccination trial to determine the immunogenicity of a trivalent CPS8-ComP, CPS9V-ComP, and CPS14-ComP pneumococcal bioconjugate vaccine (Fig. 4a-l). Three control groups were included, one group receiving carrier protein alone (unglycosylated ComP), another group receiving a monovalent vaccine of the CPS14-ComP bioconjugate to account for IgG specificity when analyzing immune responses against other serotypes, and a third group receiving Pevnar 13[®] as a positive control. All immunogen groups contained an equal mixture of Freund's adjuvant, including mice receiving

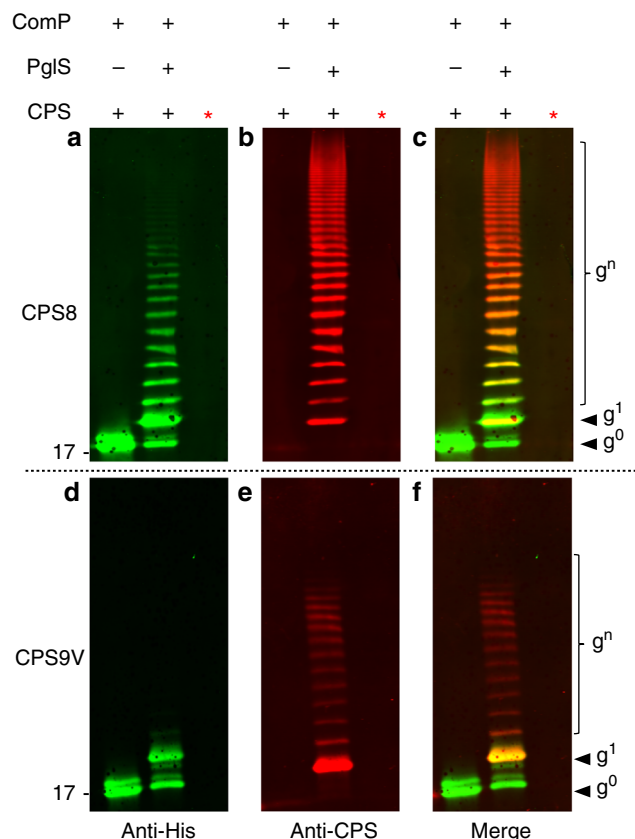


Fig. 3 Western blot analysis of CPS8-ComP and CPS9V-ComP glycoproteins. *Escherichia coli* SDB1 cells were prepared co-expressing ComP, PglS, and either the pneumococcal CSP8 or CPS9V. Affinity-purified glycosylated ComP from each strain was analyzed for protein glycosylation via western blot analysis. **a–c** Western blot analysis of CPS8-ComP bioconjugates compared against ComP alone. **a** Anti-His channel probing for Hexa-histidine-tagged ComP purified from SDB1 expressing CPS8 in the presence or absence of PglS. **b** Anti-glycan channel probing for CPS8. **c** Merged images for panels a and b. **d–f** Western blot analysis of CPS9V-ComP bioconjugates compared against ComP alone. **d** Anti-His channel probing for Hexa-histidine-tagged ComP purified from SDB1 expressing CPS9V in the presence or absence of PglS. **e** Anti-glycan channel probing for CPS9V. **f** Merged images for panels d and e. The red asterisk indicates samples that were proteinase K treated for 1 h at 55 °C. Source data are provided as a Source Data file

Pprevnar 13[®]. Day 49 sera from each group were analyzed by ELISAs on plates coated with *S. pneumoniae* serotypes 8, 9V, and 14. As mentioned above, serotypes 9V and 14 are included in Pprevnar 13[®] and an elevated IgG response could be seen in Pprevnar 13[®]-immunized mice against these two serotypes 49 days post vaccination. Mice receiving the monovalent CPS14-ComP bioconjugate also showed significant IgG increase specific to serotype 14 specific (Fig. 4i). Mice receiving the trivalent CPS8-/CPS9V-/CPS14-ComP bioconjugate all had statistically significant increases in serotype-specific IgG responses 49 days post vaccinations (Fig. 4j–l).

Because Freund's adjuvant is not a suitable adjuvant for human clinical development, we performed another immunization trial with vaccines formulated with Imject Alum Adjuvant, a mild adjuvant containing a mixture of aluminum hydroxide and magnesium hydroxide. Vaccination cohorts included a buffer/adjuvant test group, a Pprevnar 13[®] test group, and a trivalent CPS8-/CPS9V-/CPS14-ComP bioconjugate test group. Groups of three mice were vaccinated on days 1, 14, and 28. Serum was

collected on day 42 and used to determine effector functions via an opsonophagocytosis assay (OPA). Given the limited amounts of sera collected from individual mice, sera were tested for bactericidal activity against serotypes 8 and 14, as one serotype is included in Pprevnar 13[®] (serotype 14) and one is not (serotype 8). As seen in Fig. 5a, b, serum from a representative mouse vaccinated with the trivalent CPS8-/CPS9V-/CPS14-ComP bioconjugate had increased bactericidal activity against *S. pneumoniae* serotype 14 strain when compared to sera from a mock-vaccinated mouse. Importantly, that same bioconjugate vaccinated serum had high bactericidal activity against a *S. pneumoniae* serotype 8 strain, which was not observed for Pprevnar 13[®]-vaccinated sera due to the absence of this conjugate in its formulation.

Glycoengineering bioconjugates using a conventional carrier.

Up to this point, we have exploited the use of ComP from *Acinetobacter baylyi* ADP1 as a carrier protein for pneumococcal bioconjugate vaccine production; however, we sought to increase the commercial applicability of this technology by engineering a conventional vaccine carrier to be compatible with our O-linked OTase. To this end, we generated a chimeric fusion protein consisting of the ΔE553 variant of exotoxin A from *P. aeruginosa* (EPA) C terminally fused to a ComP fragment lacking its first 28 amino acids (ComPΔ28). We used a ComP ortholog from *Acinetobacter soli* strain 110264 (accession number ENV58402) as it was most efficiently glycosylated by PglS and also found to be glycosylated at the same conserved serine as ComP from *A. baylyi* ADP1 (Supplemental Fig. 6). The EPA fusion was linked to ComPΔ28 with a glycine–glycine–glycine–serine linker and trafficked to the periplasm with a DsbA signal sequence.

Because current formulations of pneumococcal conjugate vaccines do not contain a conjugate for serotype 8, we focused on generating an EPA-CPS8 pneumococcal bioconjugate. The EPA fusion was introduced into SDB1 cells co-expressing PglS and CPS8, subsequently purified, and then probed for glycosylation. As seen in Fig. 6a, b, the EPA fusion was efficiently glycosylated with CPS8 as determined by both western blot and Coomassie staining of purified glycoprotein. Furthermore, MS analysis of intact glycoproteins confirmed that the EPA fusion was repetitively modified with an increasing mass unit of 662 Da, which is the calculated mass of a single CPS8 subunit (Fig. 6c, d). The EPA fusion was found to be glycosylated with at least 11 CPS8 subunits by intact protein analysis; however, western blot and Coomassie analyses indicated that >15 subunits were able to be transferred.

Subsequently, we performed a vaccination experiment comparing the immunogenicity of an EPA-CPS8 pneumococcal bioconjugate to a ComP-CPS8 pneumococcal bioconjugate. Groups of 10 mice were either vaccinated with 5 μg of EPA alone (based on total protein), 5 μg of ComP-CPS8 (based on polysaccharide as determined by anthrone sulfuric acid), or 100 ng of EPA-CPS8 (based on polysaccharide as determined by MS of intact EPA-CPS8). Mice were vaccinated on days 1, 14, and 28 with serum collected on day 42. All vaccines were formulated 1:1 with inject Alum Adjuvant. ELISAs were subsequently performed to determine the IgG titers specific to CPS8. As seen in Fig. 7a, mice vaccinated with either ComP-CPS8 or EPA-CPS8 had statistically significant increases in IgG titers specific to CPS8 when compared to EPA-vaccinated mice. Additionally, the protective capacity of sera from vaccinated mice was determined using a murine adapted OPA with whole-blood leukocytes. As shown in Fig. 7b, sera from vaccinated mice immunized with ComP-CPS8 displayed high levels of bactericidal killing ranging from 84 to 50%, with one mouse not displaying any killing

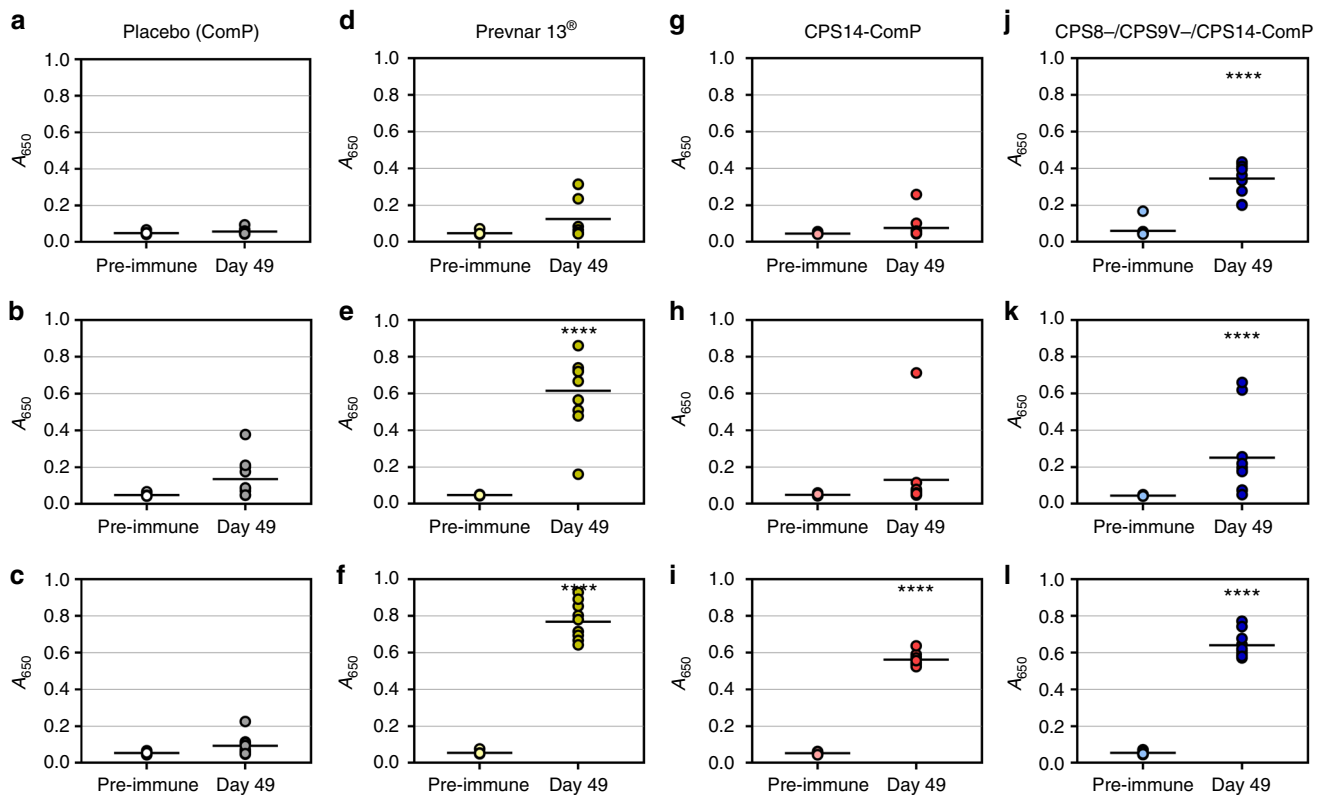


Fig. 4 Immunoglobulin G (IgG) responses of mice vaccinated with ComP, Prevnar 13[®], a monovalent bioconjugate and a trivalent bioconjugate. Groups of mice were vaccinated with ComP alone, Prevnar 13[®], a monovalent CPS14-ComP bioconjugate vaccine, or a CPS8-/CPS9V-/CPS14-ComP bioconjugate vaccine. Sera were collected on day 49 and analyzed for serotype-specific IgG responses via enzyme-linked immunosorbent assay (ELISA) compared against sera collected on day 0. **a-c** No IgG responses were detected in placebo vaccinated-mice for serotypes 8 (**a**), 9V (**b**), or 14 (**c**). **d-f** Prevnar 13[®]-vaccinated mice did not have detectable IgG responses to serotype 8 (**d**), but did have IgG responses specific to serotype 9V (**e**) and 14 (**f**). **g-i** Mice vaccinated with a CPS14-ComP bioconjugate vaccine did not have IgG responses to serotypes 8 (**g**) or 9V (**h**), but did have IgG responses to serotype 14 (**i**). **j-l** Trivalent CPS8-/CPS9V-/CPS14-ComP bioconjugate vaccinated mice all had statistically significant IgG responses to serotypes 8 (**j**), 9V (**k**), and 14 (**l**). Unpaired *t* tests (Mann-Whitney) were performed to statistically analyze pre-immune sera from day 49 sera. *P* values for each case tested were *****p* = 0.0001. Each dot represents a single vaccinated mouse (*n* = 10 mice per group). ELISA statistical calculations were performed on sera samples run in technical triplicates. Error bars indicate the standard deviation of the mean. Source data are provided as a Source Data file

activity. Moreover, sera from EPA-CPS8-vaccinated mice also displayed bactericidal ranging from 88 to 10%, with three mice displaying no killing activity. Expectedly, sera from EPA-vaccinated mice did not display killing activity.

Discussion

Traditional chemical conjugate vaccine synthesis is complex, costly, and laborious,¹⁵ therefore, new technologies to complement existing manufacturing pipelines are needed. One of these is bioconjugation, which has been thoroughly progressing as a feasible manufacturing alternative. The ability to glycosylate carrier proteins with polysaccharides containing Glc as the reducing end sugar has been elusive though, hindering the development of pneumococcal bioconjugate vaccines covering clinically relevant serotypes. Here we report the use of an *O*-linking OTase system for generating pneumococcal bioconjugate vaccines. Furthermore, we show that PglS naturally accepts polysaccharides containing Glc at the reducing end, a feat previously thought technically impossible due to substrate specificity limitations of all known conjugating enzymes.

The process of bioconjugation, described over a decade ago¹⁶, has proven to be both technically and commercially feasible. This is best evidenced by the 2015 partnership between GlaxoSmithKline and GlycoVaxyn for more than 200 million US dollars. To date, bioconjugation relies on two conjugating enzymes, PglB and PglL, with

much of the focus on PglB due to its inherent ability to glycosylate soluble proteins at a known sequon³⁰. As such, PglB has been the workhorse for the development and generation of bioconjugate vaccines in clinical trials. Examples include the Flexyn2a bioconjugate¹⁸ against *Shigella dysenteriae* as well as a tetravalent ExPEc4V bioconjugate¹⁷ vaccine against extraintestinal pathogenic *E. coli*. Recently, PglB was used to generate a bioconjugate vaccine against serotype 4 of pneumococcus³⁷. However, serotype 4 contains *N*-acetylgalactosamine as the reducing end sugar, which is one of the known substrates for PglB.

PglL also has commercially applicable features given its ability to transfer polysaccharides with Gal at the reducing end²⁵. However, until recently, PglL was thought to only glycosylate a few *Neisseria* proteins³¹, most of which were membrane-associated proteins. Research by the Wang group though has resulted in the generation of a PglL-specific sequon that can be engineered onto any carrier protein and efficiently be glycosylated by PglL, thus rendering the production of PglL-manufactured bioconjugates more practical^{38,39}. However, PglB and PglL are not useful for the production of the overwhelming majority pneumococcal serotypes due to the presence of Glc at their reducing ends.

The genome of *A. baylyi* ADP1 encodes for two *O*-OTases, a PglL ortholog, which is a general OTase, and PglS, which glycosylates a single protein, CompP²⁸. CompP is orthologous to type IV pilin proteins, like PilA from *P. aeruginosa* and PilE from

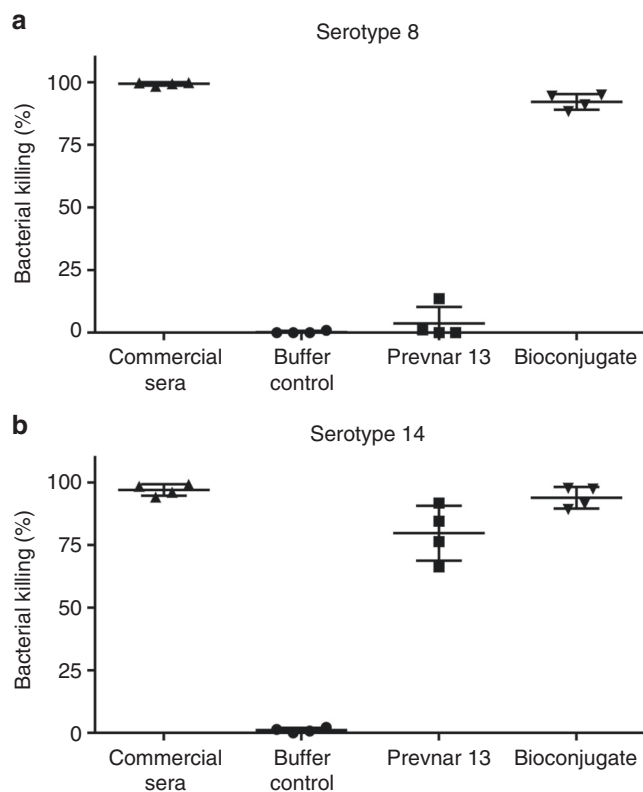


Fig. 5 Bactericidal activity of sera from vaccinated mice against *Streptococcus pneumoniae* serotypes 8 and 14. Opsonophagocytosis assays (OPAs) of sera from mice vaccinated with either buffer control ($n =$ two female mice), Pevnar 13[®] ($n =$ two female mice), or bioconjugate vaccine against both *S. pneumoniae* serotypes 8 (**a**) and 14 (**b**) ($n =$ two female mice). OPAs were performed twice in order to have two biological replicates for interpretation. Serotype-specific commercial rabbit anti-*S. pneumoniae* sera were used as positive controls. A 5% ($v v^{-1}$) sample serum and a bacterial multiplicity of infection (MOI) of 0.01 were added to fresh whole blood from naive mice to perform the assay. Viable bacterial counts were performed after 4 h of incubation. To determine bacterial killing, viable bacterial counts from tubes incubated with sample sera were compared to those incubated with control naive mouse sera. Results are expressed as percent bacterial killing for individual mice, with error bars representing the standard deviation of the mean. Source data are provided as a Source Data file

Neisseria gonorrhoeae, both of which are glycosylated by the OTases TfpO (also known as PilO)⁴⁰ and PglL (also known as PglO)⁴¹, respectively. TfpO glycosylates its cognate pilin at a C-terminal serine residue³³, which is not present in ComP. Some *Acinetobacter* strains also possess TfpO orthologs²⁸. PglL glycosylates PilE at an internal serine located at position 63 (ref. 42). ComP contains serine residues near position 63 and the surrounding residues show limited conservation to PilE from *N. gonorrhoeae*; however, Ser 63 and its surrounding residues were not part of the ComP glycosylation site. Instead, PglS glycosylates ComP at a single serine residue located at position 84, a glycosylation site which is not a canonical LCR, rich in proline, alanine, and serine residues. The ability of PglS to transfer polysaccharides containing Glc as the reducing end sugar coupled with the identification of a previously unrecognized site of glycosylation within the pilin superfamily demonstrates that PglS is a functionally distinct OTase from PglL and TfpO, and suggests that PglS belongs to a separate family of OTases.

Using the PglS/ComP OTase/acceptor protein pair, we have generated the first polyvalent pneumococcal bioconjugate vaccine

and demonstrated its immunogenicity and efficacy using correlates of protection previously established as gold standards for pneumococcal conjugate vaccines⁴³. First, we demonstrate serotype-specific IgG responses of CPS8-/CPS9V-/CPS14-ComP-vaccinated mice. In these experiments, we found that the IgG response to all serotypes tested in bioconjugate-vaccinated mice were robust as determined by ELISA. Second, we showed that serum from a mouse vaccinated with pneumococcal bioconjugate vaccine was protective based on bactericidal killing assays against serotype 8 and 14 pneumococci. In addition, we have generated the first pneumococcal bioconjugate vaccine containing a conventional vaccine carrier. Namely, we have engineered the use of a ComP fragment as a glycotag, which can be added to the C terminus of EPA. We then paired the EPA fusion with the CPS8 polysaccharide and PglS, generating the EPA-CPS8 bioconjugate, a first of its kind pneumococcal bioconjugate vaccine. The EPA-CPS8 bioconjugate vaccine elicited high IgG titers specific to serotype 8 that were protective as determined via bactericidal killing. Importantly, vaccination with as little as 100 ng of polysaccharide in the EPA-CPS8 bioconjugate was able to provide protection.

Even with the introduction and implementation of pneumococcal conjugate vaccines over the past two decades, hundreds of thousands of deaths are still attributed to pneumococcus each year¹⁰. This is due in part to the 90+ serotypes of *S. pneumoniae* and the complex manufacturing methods required to synthesize pneumococcal conjugate vaccines. Together, these factors hinder development of broader, more protective and less costly variations of the vaccines. Our bioconjugation platform for synthesizing pneumococcal conjugate vaccines from polysaccharides with Glc at the reducing end could expedite development and lower manufacturing costs. PglS-derived bioconjugates could complement existing manufacturing pipelines or completely bypass the dependency on chemical conjugation methodologies, enabling the production of a more comprehensive pneumococcal conjugate vaccine. Here we present data using the natural acceptor protein, ComP, as well as a proof-of-principle EPA fusion protein as the targets of PglS glycosylation. However, future iterations of the EPA vaccine construct will impart additional sites of glycosylation to increase the glycan to protein ratio as well as expand upon the number of serotypes in order to develop a comprehensive pneumococcal bioconjugate vaccine. Regardless, we present compelling data indicating that these pneumococcal bioconjugates have the potential for further commercial development. Importantly, the platform technology we present in this study is not limited to pneumococcal polysaccharides, but in fact, has vast applicability for generating bioconjugate vaccines for many important human and animal pathogens that are incompatible with PglB and PglL. Notable examples include the human pathogens *Klebsiella pneumoniae* and Group B *Streptococcus* as well as the swine pathogen *Streptococcus suis*, all immensely relevant pathogens with no licensed vaccines available.

Methods

Bacterial strains, plasmids, and growth condition. Strains and plasmids used in this work are listed in Supplemental Table 1. Unless otherwise stated, *E. coli* strains were grown in Terrific Broth (TB) at 37 °C overnight for ComP glycoprotein production or Super Optimal Broth (SOB) at 30 °C overnight for EPA glycoprotein production. *Streptococcus pneumoniae* strains were grown in brain heart infusion (BHI) broth or sheep blood agar plates at 37 °C in 5% CO₂. For plasmid selection, the antibiotics were used at the following concentrations: ampicillin (100 $\mu\text{g mL}^{-1}$), tetracycline (20 $\mu\text{g mL}^{-1}$), chloramphenicol (12.5 $\mu\text{g mL}^{-1}$), kanamycin (20 $\mu\text{g mL}^{-1}$), and spectinomycin (80 $\mu\text{g mL}^{-1}$) were added as needed. Oligonucleotides used in this study are listed in Supplementary Table 2.

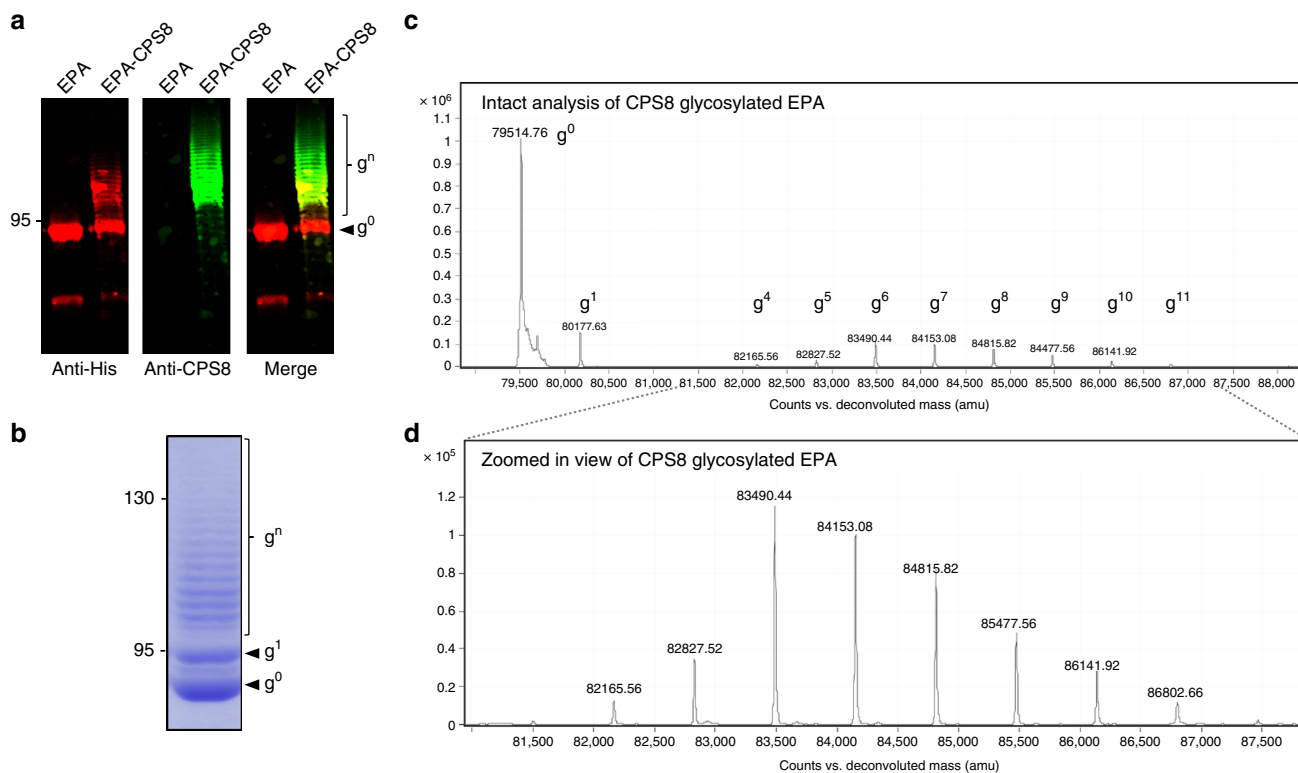


Fig. 6 Analysis of exotoxin A from *Pseudomonas aeruginosa* (EPA) glycosylation with the CPS8 capsular polysaccharide. Western blot analysis of EPA-CPS8 bioconjugates compared against EPA alone. **a** (Left panel) Anti-His channel probing for Hexa-histidine-tagged EPA purified from SDB1 expressing CPS8 in the presence or absence of PglS. **a** (Middle panel) Anti-glycan channel probing for CPS8. **a** (Right panel) Merged images for left and middle panels. **b** EPA-CPS8 separated on a SDS- polyacrylamide gel stained with Coomassie. **c, d** Intact protein mass spectrometry analysis showing the MS1 mass spectra for purified EPA-CPS8. The EPA fusion protein has a theoretical mass of 79,526.15Da and can be observed as the peak at 79,514.76 Da. The EPA fusion protein was also observed in multiple states of increasing mass corresponding to the CPS8 repeating subunit, which has a theoretical mass of 662Da. Varying glycoforms of the EPA-CPS8 were observed and are denoted by “ g^{numeric} ”, where “ g ” stands for glycoform and the “numeric” corresponds to the number of repeating CPS8 subunits. The EPA fusion protein was modified with up to 11 repeating subunits of the CPS8 glycan. Panel d provides a zoomed in view of the varying EPA-CPS8 glycoforms. Source data are provided as a Source Data file

Heterologous glycosylation in *E. coli*. *Escherichia coli* SDB1 was made electro-competent by growing cells to mid-logarithmic stage followed by two rounds of washing in 10% glycerol and a final resuspension in 1/250th of the original culture volume. Cells were electroporated with plasmids encoding the glycan synthesis loci, acceptor proteins, and OTases. Colonies were picked and grown at 37 °C in TB or SOB with appropriate antibiotic selection and immediately induced with 0.05–0.1 mM isopropyl β -D-1-thiogalactopyranoside or 0.2% arabinose as needed and left overnight at 37 °C. Cultures requiring arabinose induction received a second dose of arabinose after 4 h. Cell pellets were obtained at stationary phases and prepared for western blot analysis.

Western blotting. Cell lysates containing the equivalent of $OD_{600} = 0.1$ units were loaded on 12.5% or 7% in-house prepared sodium dodecyl sulfate-polyacrylamide gel electrophoresis (SDS-PAGE) gels, which were then transferred to nitrocellulose membranes (Bio-Rad). Western blots were employed to determine protein modification. Primary antibodies included Pneumococcus Type 8 Serum (Ref. # 16751), Pneumococcus Type 9 Serum (Ref. # 16903), and Pneumococcus Type 14 Serum (Ref. # 16751), all used at 1:1000 dilutions. Additional antibodies included 6x-His Tag Monoclonal Antibody (HIS.H8) (Catalog # MA1-21315), used at 1:1000, and anti-*Pseudomonas* exotoxin A antibody (P2318-1ML), used at 1:5000. Secondary antibodies included Licor IRDye 680RD goat anti-mouse (925-68070) and goat anti-rabbit 800CW (926-32211) used at 1:10,000 dilutions. Western blotting was performed according to our previously published protocols²⁸. Briefly, samples were separated by SDS-PAGE, transferred to nitrocellulose, blocked with Licor TBS blocking buffer, incubated with primary antibodies for 30 min, washed three times in TBS supplemented with Tween-20, incubated with secondary antibodies for 30 min, washed three times with TBS supplemented with Tween-20, and then visualized using an Odyssey Infrared Imaging System (LiCor Biosciences, USA).

Purification of proteins and glycoproteins. C terminally Hexa-histidine-tagged ComP and ComP bioconjugates were purified from *E. coli* total membrane

preparations. Cells were grown overnight in 2 L of TB at 37 °C, washed with phosphate-buffered saline (PBS) buffer, and re-suspended in 60 mL of the same buffer. Cells were lysed by two rounds of cell disruption at approximately 20 kPSI using a French press (Aminco), followed by the addition of a protease inhibitor cocktail (Roche). Lysates were centrifuged twice for 30 min at 20,000 $\times g$ to pellet cell debris. Supernatants were ultra-centrifuged at 100,000 $\times g$ for 60 mins to pellet total membranes. The pellets were re-suspended in PBS buffer containing 0.5% *n*-dodecyl- β -D-maltoside (DDM) and membrane proteins were solubilized by tumbling for 48 h. An equal volume of PBS was added to the suspension to reduce detergent concentration to 0.25% and the suspension was ultra-centrifuged at 100,000 $\times g$ for 60 mins. Solubilized membranes were filtered through 0.45 and 0.22 μ m filters and loaded on a His-Trap HP column (GE Healthcare) fitted to an ÄKTA purifier (Amersham Biosciences, Sweden). The column was equilibrated with a PBS/DDM buffer containing 20 mM imidazole prior to loading the sample. Unbound proteins were removed by washing the column with seven column volumes of buffer containing 20 and 30 mM imidazole in PBS stepwise. To elute proteins bound to the column, a gradient elution with an incremental increase in imidazole concentration was used. The majority of unconjugated and conjugated ComP eluted between 180 and 250 mM imidazole. Imidazole was removed by an overnight round of dialysis followed by two 2-h rounds through a 3.5 kDa dialysis membrane (Spectrum labs) in a 250 mL dialysis buffer composed of PBS containing 0.25% ($w v^{-1}$) DDM. The final theoretical concentration of imidazole post dialysis was about 0.007 mM. Proteins were quantified using a DC kit (Bio-Rad), after which the samples were diluted to the appropriate concentrations for mouse immunizations.

C terminally Hexa-histidine-tagged EPA fusion proteins were purified from *E. coli* lysates lysed using mechanical disruption at 35,000 PSI using a cell disruptor from Constant Systems. Lysates were clarified at 15,000 $\times g$ for 30 min. The supernatants were passed over 3 mL of nickel NTA agarose, washed with 10 column volumes of buffer containing 20 mM Tris, 10 mM imidazole, 500 mM NaCl, pH 8.0, and eluted with the same buffer containing 300 mM imidazole. Eluted proteins were concentrated using an Amicon Ultra-15 concentrator,

Primers used are listed in Supplemental Table 2. PCR reactions were performed using *Pfu* polymerase and 2–10 ng of pMN2 as template. The PCR reaction consisted of an initial denaturation of 30 s at 95 °C followed by 16 cycles of 30 s at 95 °C, 60 s at 55 °C, 360 s at 68 °C with no final extension. PCR reactions were *DpnI* digested for 2 h to remove the template plasmid, then transformed into electro-competent DH5a cells, and grown on ampicillin for plasmid selection. Colonies were sequenced to confirm mutagenesis.

Digestion of ComP-CPS14 conjugate. CPS14-ComP was affinity purified and separated via SDS-PAGE and Coomassie stained. SDS-PAGE separated CPS14-ComP bands were excised and destained in a 50:50 solution of 50 mM NH_4HCO_3 :100% ethanol for 20 min at room temperature with shaking at 750 rpm. Destained bands were then washed with 100% ethanol, vacuum dried for 20 min, and rehydrated in 10 mM dithiothreitol (DTT) in 50 mM NH_4HCO_3 . Reduction was carried out for 60 min at 56 °C with shaking. The reducing buffer was then removed and the gel bands washed twice in 100% ethanol for 10 min to ensure the removal of remaining DTT. Reduced ethanol washed samples were sequentially alkylated with 55 mM iodoacetamide in 50 mM NH_4HCO_3 in the dark for 45 min at room temperature. Alkylated samples were then washed with two rounds of Milli-Q water and 100% ethanol then vacuum dried. Alkylated samples were then rehydrated with 10 ng μl^{-1} GluC (Promega, Madison, WI, USA) in 40 mM NH_4HCO_3 at 4 °C for 1 h. Excess GluC was removed, gel pieces were covered in 40 mM NH_4HCO_3 , and incubated for 24 h at 37 °C. Peptides were concentrated and desalted using C_{18} stage tips^{44,45} and stored on tip at 4 °C. Peptides were eluted in Buffer B (0.5% acetic acid, 80% MeCN) and dried before analysis by liquid chromatography-mass spectrometry (LC-MS).

Reversed phase LC-MS and HCD MS-MS. Purified peptides were re-suspended in Buffer A* and separated using an in-house packaged 25 cm, 75 μm inner diameter, 360 μm outer diameter, 1.7 μm 130 Å CSH C_{18} (Waters, Manchester, UK) reverse-phase analytical column with an integrated HF-etched nESI tip. Samples were loaded directly onto the column using an ACQUITY UPLC M-Class System (Waters) at 600 nL min⁻¹ for 20 min with Buffer A (0.1% formic acid (FA)) and eluted at 300 nL min⁻¹ using a gradient altering the concentration of Buffer B (99.9% acetonitrile, 0.1% FA) from 2 to 32% B over 60 min, then from 32 to 40% B in the next 10 min, then increased to 80% B over 8 min period, held at 100% B for 2 min, and then dropped to 2% B for another 10 min. Reverse-phase separated peptides were infused into a Q-Exactive (Thermo Scientific) mass spectrometer and data acquired using data-dependent acquisition. Two methods were used to identify putative glycopeptides. Method A aimed to enable robust peptide identification in which one full precursor scan (resolution 70,000; 350–1850 m/z , AGC target of 1×10^6) was followed by 10 data-dependent higher energy collisional dissociation (HCD) MS-MS events (resolution 35k AGC target of 1×10^5 with a maximum injection time of 110 ms, NCE 26 with 25% stepping) with 90 s dynamic exclusion enabled. Method B aimed to enable more complete characterization of glycans within glycopeptides with one full precursor scan (resolution 70,000; 350–1850 m/z , AGC target of 1×10^6) followed by 10 data-dependent HCD MS-MS events (resolution 35k AGC target of 5×10^5 with a maximum injection time of 250 ms, NCE 13 with 25% stepping) with 90 s dynamic exclusion enabled.

Database interrogation of identified glycopeptides. Raw files were processed manually to identify potential glycopeptides based on the diagnostic oxonium 204.08 m/z ion. Putative glycopeptide-derived scans were manually inspected and identified as possible GluC-derived ComP glycopeptides based on the presence of an intense deglycosylated ComP-derived peptide ion, matching within 10 ppm using the ExPasy FindPept tool (<https://web.expasy.org/findpept/>). To facilitate peptide assignments, the resulting glycopeptides were manually annotated according to ref.⁴⁶ with the aid of the Protein Prospector tool MS-Product (<http://prospector.ucsf.edu/prospector/cgi-bin/msform.cgi?form = msproduct>).

Intact protein analysis. Intact analysis was performed using a 6520 Accurate Mass Quadrupole Time-of-Flight mass spectrometer (Agilent, Santa Clara, CA, USA). Protein samples were re-suspended in 2% ACN, 0.1% trifluoroacetic acid, and immediately loaded onto a C5 Jupiter 5 μm 300 Å 50 mm \times 2.1 mm column (Phenomenex, Torrance, CA, USA) using an Agilent 1200. Samples were desalted by washing with buffer A (2% ACN, 0.1% FA) for 4 min and then separated with a 12 min linear gradient from 2 to 100% buffer B (80% ACN, 0.1% FA) at a flow rate of 0.200 mL min⁻¹. MS1 mass spectra were acquired at 1 Hz between a mass range of 300–3000 m/z . Intact mass analysis and deconvolution was performed using MassHunter B.06.00 (Agilent).

Opsonophagocytosis assay. The assays were performed as previously described^{47,48} and are briefly described below. **Blood collection.** Blood was collected by intracardiac puncture from naive female mice (Charles River, Wilmington, MA, USA), treated with sodium heparin, then diluted to obtain 6.25×10^6 leukocytes mL⁻¹ in RPMI-1640 supplemented with 5% heat-inactivated fetal bovine serum, 10 mM HEPES, 2 mM L-glutamine, and 50 μM 2-mercaptoethanol. All reagents were from Gibco (Invitrogen, Burlington, ON, Canada). **Bacterial suspension preparation.** Isolated colonies on sheep blood agar plates of either *S.*

pneumoniae serotypes 8 or 14 (Statens Serum Institut, Denmark) were inoculated in 5 mL of Todd–Hewitt Broth (THB) (Oxoid, Thermo Fisher Scientific, Nepean, Canada) and incubated for 16 h at 37 °C with 5% CO_2 . Working cultures were prepared by transferring 0.1 mL of 16 h cultures into 10 mL of THB, which was then incubated for 5 h. Bacteria were washed three times and re-suspended in PBS to obtain an OD₆₀₀ value of 0.6, which corresponds to 1.5×10^8 and colony-forming units (CFU) mL⁻¹ and to 3.5×10^8 CFU mL⁻¹ for serotype 8 and serotype 14, respectively. Final bacterial suspensions were prepared in complete cell culture medium to obtain a concentration of 6.25×10^4 CFU mL⁻¹. The number of CFU mL⁻¹ in the final suspensions was determined by plating samples onto Todd–Hewitt agar (THA). **Opsonophagocytosis Assay.** Diluted whole blood (5×10^5 total leukocytes) was mixed with 5×10^3 CFU of *S. pneumoniae* serotype 8 or 14 (multiplicity of infection of 0.01) and 5% (v/v) of serum from control (placebo) or vaccinated mice in a microtube to a final volume of 0.2 mL. Microtubes were incubated for 4 h at 37 °C with 5% CO_2 , with shaking. After incubation, viable bacterial counts were performed on THA. Tubes with the addition of naive mouse sera or commercial rabbit anti-*S. pneumoniae* types 8 or 14 serum (Statens Serum Institut, Denmark) were used as negative and positive controls, respectively. The percentage of bacterial killing was determined using the following formula: percent bacteria killed = $[1 - (\text{bacteria recovered from sample tubes} / \text{bacteria recovered from negative control tubes with naive sera})] \times 100$.

Reporting summary. Further information on experimental design is available in the Nature Research Reporting Summary linked to this article.

Data availability

The authors declare that data supporting the findings of this study are available within the paper and its supplemental files. The source data underlying Figs. 1, 3, 4, 5, 6, 7 and supplemental Figs. 2 and 5 are provided as a Source Data file.

Received: 7 August 2018 Accepted: 5 February 2019

Published online: 21 February 2019

References

- Hausdorff, W. P., Hoet, B. & Adegbola, R. A. Predicting the impact of new pneumococcal conjugate vaccines: serotype composition is not enough. *Expert. Rev. Vaccin.* **14**, 413–428 (2015).
- O'Brien, K. L. et al. Burden of disease caused by *Streptococcus pneumoniae* in children younger than 5 years: global estimates. *Lancet* **374**, 893–902 (2009).
- WHO. *Estimated Hib and Pneumococcal Deaths for Children under 5 years of Age*, 2008. http://www.who.int/immunization/monitoring_surveillance/burden/estimates/Pneumo_hib/en (2013).
- CDC. *Pneumococcal Disease*. <https://www.cdc.gov/pneumococcal/vaccination.html> (2017).
- Cadoz, M. Potential and limitations of polysaccharide vaccines in infancy. *Vaccine* **16**, 1391–1395 (1998).
- Avci, F. Y., Li, X., Tsuji, M. & Kasper, D. L. A mechanism for glycoconjugate vaccine activation of the adaptive immune system and its implications for vaccine design. *Nat. Med.* **17**, 1602–1609 (2011).
- Pollard, A. J., Perrett, K. P. & Beverley, P. C. Maintaining protection against invasive bacteria with protein–polysaccharide conjugate vaccines. *Nat. Rev. Immunol.* **9**, 213–220 (2009).
- CDC. *Vaccines for Children Program (VFC)*. <https://www.cdc.gov/vaccines/programs/vfc/awardees/vaccine-management/price-list/index.html> (2018).
- Pfizer. *Pfizer Inc. 2017 Financial Report*. <https://www.sec.gov/Archives/edgar/data/78003/000007800318000027/pfe-exhibit13x12312017x10k.htm> (2017).
- Wahl, B. et al. Burden of *Streptococcus pneumoniae* and *Haemophilus influenzae* type b disease in children in the era of conjugate vaccines: global, regional, and national estimates for 2000–15. *Lancet Glob. Health* **6**, e744–e757 (2018).
- Loo, J. D. et al. Systematic review of the effect of pneumococcal conjugate vaccine dosing schedules on prevention of pneumonia. *Pediatr. Infect. Dis. J.* **33**, S140–S151 (2014).
- Grabenstein, J. D. & Musey, L. K. Differences in serious clinical outcomes of infection caused by specific pneumococcal serotypes among adults. *Vaccine* **32**, 2399–2405 (2014).
- Cui, Y. A., Patel, H., O'Neil, W. M., Li, S. & Saddier, P. Pneumococcal serotype distribution: a snapshot of recent data in pediatric and adult populations around the world. *Hum. Vaccin. Immunother.* **13**, 1–13 (2017).
- Gladstone, R. A. et al. Five winters of pneumococcal serotype replacement in UK carriage following PCV introduction. *Vaccine* **33**, 2015–2021 (2015).
- Frasch, C. E. Preparation of bacterial polysaccharide–protein conjugates: analytical and manufacturing challenges. *Vaccine* **27**, 6468–6470 (2009).

16. Feldman, M. F. et al. Engineering N-linked protein glycosylation with diverse O antigen lipopolysaccharide structures in *Escherichia coli*. *Proc. Natl. Acad. Sci. USA* **102**, 3016–3021 (2005).
17. Huttner, A. et al. Safety, immunogenicity, and preliminary clinical efficacy of a vaccine against extraintestinal pathogenic *Escherichia coli* in women with a history of recurrent urinary tract infection: a randomised, single-blind, placebo-controlled phase 1b trial. *Lancet Infect. Dis.* **17**, 528–537 (2017).
18. Riddle, M. S. et al. Safety and immunogenicity of a candidate bioconjugate vaccine against *Shigella flexneri* 2a administered to healthy adults: a single-blind, randomized phase I study. *Clin. Vaccin. Immunol.* **23**, 908–917 (2016).
19. Nothaft, H. & Szymanski, C. M. Protein glycosylation in bacteria: sweeter than ever. *Nat. Rev. Microbiol.* **8**, 765–778 (2010).
20. Iwashkiw, J. A., Voza, N. F., Kinsella, R. L. & Feldman, M. F. Pour some sugar on it: the expanding world of bacterial protein O-linked glycosylation. *Mol. Microbiol.* **89**, 14–28 (2013).
21. Geno, K. A. et al. Pneumococcal capsules and their types: past, present, and future. *Clin. Microbiol. Rev.* **28**, 871–899 (2015).
22. Iwashkiw, J. A. et al. Exploiting the *Campylobacter jejuni* protein glycosylation system for glycoengineering vaccines and diagnostic tools directed against brucellosis. *Microb. Cell Fact.* **11**, 13 (2012).
23. Ciocchini, A. E. et al. Development and validation of a novel diagnostic test for human brucellosis using a glyco-engineered antigen coupled to magnetic beads. *PLoS Negl. Trop. Dis.* **7**, e2048 (2013).
24. Wacker, M. et al. Substrate specificity of bacterial oligosaccharyltransferase suggests a common transfer mechanism for the bacterial and eukaryotic systems. *Proc. Natl. Acad. Sci. USA* **103**, 7088–7093 (2006).
25. Faridmoayer, A. et al. Extreme substrate promiscuity of the *Neisseria* oligosaccharyl transferase involved in protein O-glycosylation. *J. Biol. Chem.* **283**, 34596–34604 (2008).
26. Faridmoayer, A., Fentabil, M. A., Mills, D. C., Klassen, J. S. & Feldman, M. F. Functional characterization of bacterial oligosaccharyltransferases involved in O-linked protein glycosylation. *J. Bacteriol.* **189**, 8088–8098 (2007).
27. Bentley, S. D. et al. Genetic analysis of the capsular biosynthetic locus from all 90 pneumococcal serotypes. *PLoS Genet.* **2**, e31 (2006).
28. Harding, C. M. et al. *Acinetobacter* strains carry two functional oligosaccharyltransferases, one devoted exclusively to type IV pilin, and the other one dedicated to O-glycosylation of multiple proteins. *Mol. Microbiol.* **96**, 1023–1041 (2015).
29. Ihssen, J. et al. Increased efficiency of *Campylobacter jejuni* N-oligosaccharyltransferase PglB by structure-guided engineering. *Open Biol.* **5**, 140227 (2015).
30. Kowarik, M. et al. Definition of the bacterial N-glycosylation site consensus sequence. *EMBO J.* **25**, 1957–1966 (2006).
31. Vik, A. et al. Broad spectrum O-linked protein glycosylation in the human pathogen *Neisseria gonorrhoeae*. *Proc. Natl. Acad. Sci. USA* **106**, 4447–4452 (2009).
32. Scott, N. E. et al. Diversity within the O-linked protein glycosylation systems of *Acinetobacter* species. *Mol. Cell. Proteom.* **13**, 2354–2370 (2014).
33. Comer, J. E., Marshall, M. A., Blanch, V. J., Deal, C. D. & Castric, P. Identification of the *Pseudomonas aeruginosa* 1244 pilin glycosylation site. *Infect. Immun.* **70**, 2837–2845 (2002).
34. Wuorimaa, T. et al. Avidity and subclasses of IgG after immunization of infants with an 11-valent pneumococcal conjugate vaccine with or without aluminum adjuvant. *J. Infect. Dis.* **184**, 1211–1215 (2001).
35. Soininen, A., Seppala, I., Nieminen, T., Eskola, J. & Kayhty, H. IgG subclass distribution of antibodies after vaccination of adults with pneumococcal conjugate vaccines. *Vaccine* **17**, 1889–1897 (1999).
36. Pilishvili, T. et al. Sustained reductions in invasive pneumococcal disease in the era of conjugate vaccine. *J. Infect. Dis.* **201**, 32–41 (2010).
37. Herbert, J. A. et al. Production and efficacy of a low-cost recombinant pneumococcal protein polysaccharide conjugate vaccine. *Vaccine* **36**, 3809–3819 (2018).
38. Pan, C. et al. Biosynthesis of conjugate vaccines using an O-linked glycosylation system. *mBio* **7**, e00443–00416 (2016).
39. Sun, P. et al. Design and production of conjugate vaccines against *S. paratyphi* A using an O-linked glycosylation system in vivo. *NPJ Vaccin.* **3**, 4 (2018).
40. Castric, P. *pilO*, a gene required for glycosylation of *Pseudomonas aeruginosa* 1244 pilin. *Microbiology* **141**, 1247–1254 (1995).
41. Aas, F. E., Vik, A., Vedde, J., Koomey, M. & Egge-Jacobsen, W. *Neisseria gonorrhoeae* O-linked pilin glycosylation: functional analyses define both the biosynthetic pathway and glycan structure. *Mol. Microbiol.* **65**, 607–624 (2007).
42. Aas, F. E. et al. *Neisseria gonorrhoeae* type IV pili undergo multisite, hierarchical modifications with phosphoethanolamine and phosphocholine requiring an enzyme structurally related to lipopolysaccharide phosphoethanolamine transferases. *J. Biol. Chem.* **281**, 27712–27723 (2006).
43. Plotkin, S. A. Correlates of protection induced by vaccination. *Clin. Vaccin. Immunol.* **17**, 1055–1065 (2010).
44. Ishihama, Y., Rappsilber, J. & Mann, M. Modular stop and go extraction tips with stacked disks for parallel and multidimensional peptide fractionation in proteomics. *J. Proteome Res.* **5**, 988–994 (2006).
45. Rappsilber, J., Mann, M. & Ishihama, Y. Protocol for micro-purification, enrichment, pre-fractionation and storage of peptides for proteomics using StageTips. *Nat. Protoc.* **2**, 1896–1906 (2007).
46. Roepstorff, P. & Fohlman, J. Proposal for a common nomenclature for sequence ions in mass spectra of peptides. *Biomed. Mass Spectrom.* **11**, 601 (1984).
47. Goyette-Desjardins, G., Roy, R. & Segura, M. Murine whole-blood opsonophagocytosis assay to evaluate protection by antibodies raised against encapsulated extracellular bacteria. *Methods Mol. Biol.* **1331**, 81–92 (2015).
48. Price, N. L. et al. Glycoengineered outer membrane vesicles: a novel platform for bacterial vaccines. *Sci. Rep.* **6**, 24931 (2016).
49. Kay, E. J., Yates, L. E., Terra, V. S., Cuccui, J. & Wren, B. W. Recombinant expression of *Streptococcus pneumoniae* capsular polysaccharides in *Escherichia coli*. *Open Biol.* **6**, 150243 (2016).

Acknowledgements

We would like to thank Brendan Wren and Laura Yates for providing the pB-8 plasmid⁴⁹. We would like to thank Andrew Webb from Walter Eliza Hall institute of medical research for providing mass spectrometry support for the peptide-based analysis. We would also like to thank the Melbourne Mass Spectrometry and Proteomics Facility of The Bio21 Molecular Science and Biotechnology Institute at The University of Melbourne for the support, maintenance, and access to mass spectrometry infrastructure for intact protein-based analysis. This work was funded by National Institute for Allergy and Infectious Disease (NIAID) R41 AI131742 grant awarded to M.F.F. and VaxNewMo. This work was partially supported by National Health and Medical Research Council of Australia (NHMRC) project grants awarded to N.E.S. (APP1100164). N.E.S. was supported by an Overseas (Biomedical) Fellowship (APP1037373) and a University of Melbourne Early Career Researcher Grant Scheme (Proposal number 603107). J.P.H. was supported by a National Science Foundation Graduate Research Fellowship (DGE-1143954), R.L.K. was supported by a Potts Memorial Foundation Postdoctoral Fellowship, and C.L.S. was supported by a Burroughs Wellcome Fund Investigators in the Pathogenesis of Infectious Disease award.

Author contributions

C.M.H., M.A.N., N.E.S., G.G.-D., H.N., A.E.M., S.M.C., J.P.H., R.L.K., all performed experiments related to this study. M.A.N., C.M.H., N.E.S. and M.F.F. analyzed data sets. C.M.S., C.L.S., M.S. and M.F.F. directed the study. C.M.H., M.A.N., and M.F.F. wrote the manuscript.

Additional information

Supplementary Information accompanies this paper at <https://doi.org/10.1038/s41467-019-08869-9>.

Competing interests: The authors declare no competing interests.

Reprints and permission information is available online at <http://npg.nature.com/reprintsandpermissions/>

Journal peer review information: *Nature Communications* thanks the anonymous reviewers for their contribution to the peer review of this work. Peer reviewer reports are available.

Publisher's note: Springer Nature remains neutral with regard to jurisdictional claims in published maps and institutional affiliations.



Open Access This article is licensed under a Creative Commons Attribution 4.0 International License, which permits use, sharing, adaptation, distribution and reproduction in any medium or format, as long as you give appropriate credit to the original author(s) and the source, provide a link to the Creative Commons license, and indicate if changes were made. The images or other third party material in this article are included in the article's Creative Commons license, unless indicated otherwise in a credit line to the material. If material is not included in the article's Creative Commons license and your intended use is not permitted by statutory regulation or exceeds the permitted use, you will need to obtain permission directly from the copyright holder. To view a copy of this license, visit <http://creativecommons.org/licenses/by/4.0/>.

© The Author(s) 2019